Centimeter-Scale Above-Room-Temperature Ferromagnetic Fe_3GaTe_2 Thin Films by Molecular Beam Epitaxy

Taikun Wang(王太坤)[1,2†], Yongkang Xu(徐永康)[1,2†], Yu Liu(刘宇)[1,2], Xingze Dai(代兴泽)[1,2], Pengfei Yan(闫鹏飞)[1,2], Jin Wang(王瑾)[1,2], Shuanghai Wang (王双海)[1,2], Yafeng Deng(邓亚丰)[1,2], Kun He(何坤)[1,2], Caitao Li(李彩涛)[1,2], Ziang Wang(王子昂)[1], Wenqin Zou(邹文琴)[3], Rongji Wen(温荣吉)[4], Yufeng Hao(郝玉峰)[4], and Liang He(何亮)[1,2*]

[1]*School of Electronic Science and Engineering, Nanjing University, Nanjing 210000, China*
[2]*National Key Laboratory of Spintronics, Nanjing University, Suzhou 215163, China*
[3]*Department of Physics, Nanjing University, Nanjing 210000, China*
[4]*College of Engineering and Applied Science, Nanjing University, Nanjing 210000, China*

(Received 22 July 2024; accepted manuscript online 10 September 2024)

Fe_3GaTe_2, as a layered ferromagnetic material, has a Curie temperature (T_c) higher than room temperature, making it the key material in next-generation spintronic devices. To be used in practical devices, large-sized high-quality Fe_3GaTe_2 thin films need to be prepared. Here, the centimeter-scale thin film samples with high crystal quality and above-room-temperature ferromagnetism with strong perpendicular magnetic anisotropy were prepared by molecular beam epitaxy technology. Furthermore, the T_c of the samples raises as the film thickness increases, and reaches 367 K when the film thickness is 60 nm. This study provides material foundations for the new generation of van der Waals spintronic devices and paves the way for the commercial application of Fe_3GaTe_2.

DOI: 10.1088/0256-307X/41/10/107502

The exploration and discovery of two-dimensional (2D) ferromagnetic materials are key to the next-generation spintronic devices.[1–5] In the past decade, various 2D ferromagnetic materials have been discovered, such as CrI_3,[6–8] $Cr_2Ge_2Te_6$,[9–11] Fe_3GeTe_2,[12–14] and $CrTe_2$.[15–17] Yet, to be used in realistic devices, ferromagnetism well above room temperatures is highly desired. Recently, a new two-dimensional ferromagnetic material Fe_3GaTe_2 has been reported with T_c of about 380 K.[18] However, all reported thin-layer Fe_3GaTe_2 samples were prepared by mechanical peeling and transferring techniques from bulk materials, with a characteristic size of tens of μm.[19–22] Therefore, the preparation of large-scale high-quality Fe_3GaTe_2 thin films is of great significance.

In this work, a series of centimeter-scale Fe_3GaTe_2 thin films with the thicknesses ranging from 22 nm to 60 nm were prepared on GaAs (111)B substrates by molecular beam epitaxy (MBE) technology. All the samples show ferromagnetism above room temperate based on magneto-transport measurements. More importantly, the T_c (334 K at 22 nm to 367 K at 60 nm) shows a positive correlation with the thicknesses of the films. Our findings provide a pathway for the large-scale preparation of Fe_3GaTe_2 thin films, which can be integrated into next-generation storage devices or spintronic devices, and serves as a reference for specific process parameters.

The Fe_3GaTe_2 crystal has a hexagonal structure with a space group of $P6_3/mmc$ and lattice parameters of $a = b = 3.9860$ Å, $c = 16.2290$ Å, $\alpha = \beta = 90°$, $\gamma = 120°$ as shown in Fig. 1(a).[18] Each unit cell consists of two Fe_3GaTe_2 layers and a van der Waals gap. In each layer, the atoms are arranged in the order of Te–Fe_{II}–Fe_IGa–Fe_{II}–Te along the *c*-axis. The Fe_IGa atomic slabs in the two layers are oppositely arranged, as indicated by the arrows in Fig. 1(a).

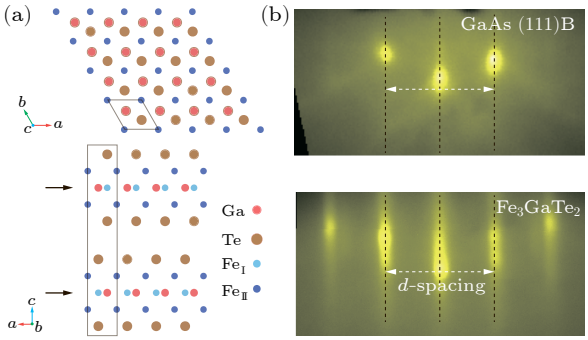

Fig. 1. (a) Structure diagram of Fe_3GaTe_2. (b) *In situ* reflection high energy electron diffraction (RHEED) images of the Fe_3GaTe_2 film and the GaAs (111)B substrate.

The growth process of the samples was monitored by RHEED and the details about growth process are shown at Note 1 of the Supplementary Material. Figure 1(b) demonstrates the RHEED pattern of the GaAs (111)B substrate

†These authors contributed equally to this work.
*Corresponding author. Email: heliang@nju.edu.cn
© 2024 Chinese Physical Society and IOP Publishing Ltd

with the diffraction dots on an arch and Kikuchi lines, presenting the high crystal quality of the substrate. After growth, sharp streaky patterns of Fe_3GaTe_2 could be observed, as shown in Fig. 1(b), which exhibits a flat surface morphology. In addition, the lattice constant of the as-grown Fe_3GaTe_2 can be extracted from the d-spacing of the substrate, ∼0.4 nm, which is consistent with the previous reports.[18]

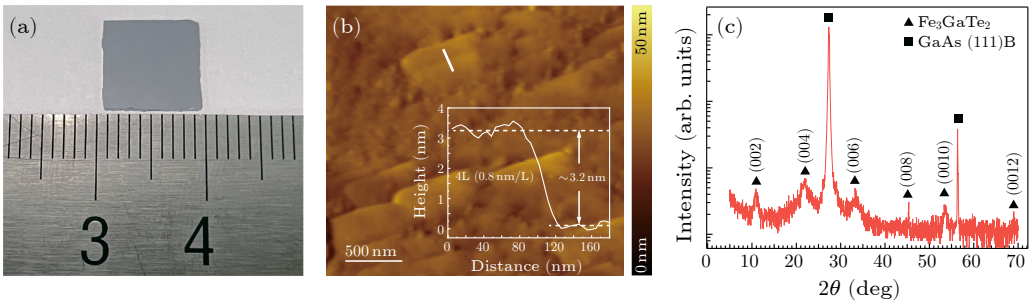

Fig. 2. (a) Optical image of a centimeter-scale Fe_3GaTe_2 thin film. (b) Atomic force microscope (AFM) image of an as-grown Fe_3GaTe_2 thin film. The inset displays the height profile along the white line. (c) X-ray diffraction spectrum of a 22 nm Fe_3GaTe_2.

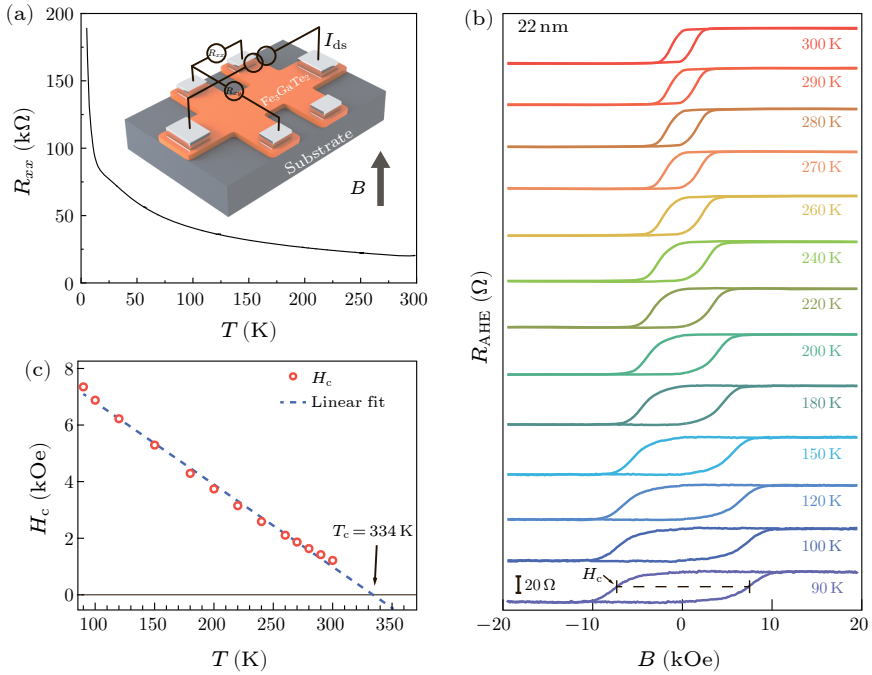

Fig. 3. (a) R_{xx} of a 22 nm Fe_3GaTe_2 thin film vs temperature, showing a semiconductor property. The inset shows the schematic diagram of the Fe_3GaTe_2 Hall bar device. (b) Anomalous Hall resistance ($R_{AHE} = R_{xy} - R_0H$) of a 22 nm Fe_3GaTe_2 film at different temperatures. Clear hysteresis loops can be observed up to room temperate. (c) Temperature-dependent H_c of a 22 nm Fe_3GaTe_2 thin film. The Curie temperature of 334 K can be estimated by a linear fit.

An optical image of a centimeter-scale Fe_3GaTe_2 film is shown in Fig. 2(a). The surface morphology of the as-grown Fe_3GaTe_2 films was characterized by an AFM, as shown in Fig. 2(b). Typical triangular terraces with a size of about 500 nm exist on the surface, which correspond to the space group of $P6_3/mmc$. The height profile of the white line is shown in the inset of Fig. 2(b). The step height shows about 3.2 nm, which matches the thickness of four Fe_3GaTe_2 layers.

As shown in Fig. 2(c), the x-ray diffraction result of the as-grown Fe_3GaTe_2 film demonstrates a distinct (001) orientation, with no other phases. The lattice parameter c is calculated to be 16.24 Å, which is similar to the reported value of 16.229 Å.[18]

In addition, the composition of Fe_3GaTe_2 films was characterized by x-ray photoelectron spectroscopy (XPS), as shown in Note 2 of the Supplementary Material. The valence states of iron (Fe), gallium (Ga), and tellurium (Te) can be found to be Fe^0 and Fe^{3+}, Ga^{2-}, and Te^{2-}, respectively. Compared to the typical valence states of Fe (Fe^{2+} and Fe^{3+}) in Fe_3GeTe_2 crystals ($T_c \sim 205$ K), the presence of Fe^0 with high spin dynamics may be one of the factors contributing to the increase in Curie temperature in Fe_3GaTe_2.[18]

After growth, the Fe_3GaTe_2 thin films have been fabricated into standard Hall bar devices by ion beam etching

(IBE) with a hard mask. The devices were connected to a transport measurement system using conductive silver paste and gold wires. The schematic diagram of the device is shown in the inset of Fig. 3(a). During the measurements, the Keithley 6221 was used as an alternating-current source with a magnitude of 1 μA and a frequency of 13 Hz. The V_{xx} and V_{xy} signals were obtained using lock-in amplifiers (SR830). Additionally, an out-of-plane magnetic field up to 2 Tesla was applied.

The R_{xx}–T curve of a 22 nm Fe_3GaTe_2 film is shown in Fig. 3(a). The resistance increases with decreasing temperature, exhibiting a semiconductor property. Note 3 of the Supplementary Material demonstrates the modified Arrott-plot with $\ln \rho/T$ vs $1/T$ in the temperature range of 95–300 K. An activation energy of 22.35 meV could be obtained through a linear fitting.

Typically, the relationship between R_{xy} and the magnetic field follows the empirical equation

$$R_{xy} = R_0 H + R_A M(H),$$

where the $R_0 H$ comprises the ordinary Hall effect, and the $R_A M$ comprises the anomalous Hall effect (AHE). The empirical equation is used to calculate the anomalous Hall resistance [$R_{AHE} = R_{xy} - R_0 H = R_A M(H)$] and to study its formation mechanism. Figure 3(b) shows the anomalous Hall resistance (R_{AHE}) of the 22 nm Fe_3GaTe_2 film at different temperatures. Clear hysteresis loops could be observed up to 300 K, which indicates that Fe_3GaTe_2 films exhibit perpendicular magnetic anisotropy (PMA) at room temperature. The extraction of the R_{AHE} from the raw R_{xy} date is shown in Note 4 of the Supplementary Material.

For ferromagnetic materials, the magnetic field corresponding to $R_{AHE} = 0\,\Omega$ was defined as the coercivity (H_c). By plotting H_c at different temperatures, a linear relationship can be found, as shown in Fig. 3(c). From the fitting, it can be estimated that H_c will reach zero at 334 ± 5 K. This temperature can be approximately considered as the Curie temperature of the 22 nm Fe_3GaTe_2 thin film.

Furthermore, Fe_3GaTe_2 thin films of different thicknesses were prepared by MBE and studied by magneto transport measurements, as shown in Fig. 4. As the same as the 22 nm sample, all the thicker films demonstrate clear anomalous Hall effect, which indicate the above-room-temperature ferromagnetism with PMA. Moreover, Fe_3GaTe_2 thin films with thickness of 60 nm were tested by high-temperature transport (290–360 K), as shown in Fig. 4(c). It can be seen from the figure that the 60 nm Fe_3GaTe_2 thin film exhibits a clear rectangular hysteresis loop at 290 K–360 K. With the rise in temperature, H_c gradually decreases, and the ferromagnetism still exists at 360 K, as shown in Fig. 4(c).

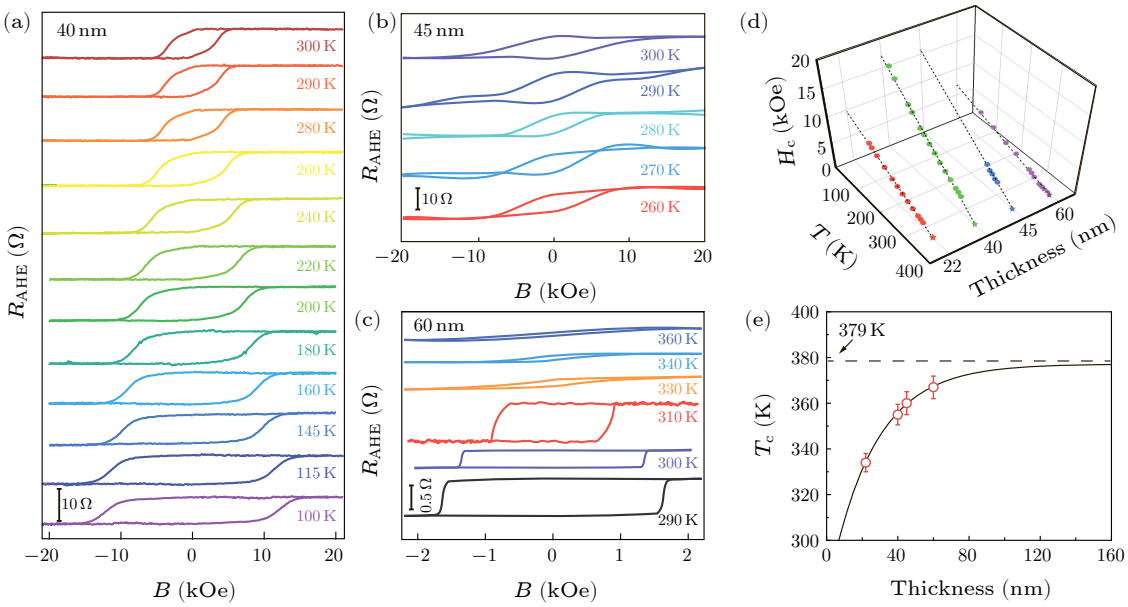

Fig. 4. Magneto-transport measurements of Fe_3GaTe_2 thin films at different temperatures with thicknesses of 40 nm (a), 45 nm (b), and 60 nm (c). Ferromagnetism can be found in the 60 nm sample up to 360 K. (d) Temperature-dependent H_c of the Fe_3GaTe_2 thin films with different thicknesses. T_c could be estimated by linear fittings as 355 K, 360 K, and 367 K, respectively. (e) The thickness-dependent T_c, from which the highest T_c of the 2D Fe_3GaTe_2 can be estimated to be 379 K.

The temperature-dependent H_c's of all the samples with different thicknesses are plotted in Fig. 4(d), and fitted by linear lines. The T_c values at various thicknesses are determined by the interception with the horizontal axis, which are 355 K, 360 K, and 367 K, respectively. The thickness-dependent T_c is shown in Fig. 4(e), which shows positively correlation between thickness and T_c. Furthermore, the highest T_c of the 2D Fe_3GaTe_2 can be esti-

mated to be about 379 K, which is similar with the previous report.[18]

In summary, a series of centimeter-size above-room-temperature ferromagnetic Fe_3GaTe_2 thin films have been grown using MBE technology, which exhibits intrinsic ferromagnetism and strong PMA. Furthermore, as the film thickness increases from 22 nm to 60 nm, the Curie temperature increases from 334 K to 367 K. Owing to the ferromagnetism above room temperature and strong PMA, Fe_3GaTe_2 thin films grown by MBE offer considerable potential for being stacked with various other 2D materials to realize the fabrication of next-generation spintronic or storage devices.

Acknowledgements. This work was supported by the National Natural Science Foundation of China (Grant No. 12241403), and the Natural Science Foundation of Jiangsu Province of China (Grant No. BK20140054).

References

[1] Guan M, Wang L, Zhao S, Zhou Z, Dong G, Su W, Min T, Ma J, Hu Z, Ren W, Ye Z G, Nan C W, and Liu M 2018 *Adv. Mater.* **30** 1802902
[2] Jin W, Zhang G J, Wu H, Yang L, Zhang W F, and Chang H X 2023 *Chin. Phys. Lett.* **40** 057301
[3] Kim S K, Beach G S D, Lee K J, Ono T, Rasing T, and Yang H 2022 *Nat. Mater.* **21** 24
[4] Wu Y, Wang W, Pan L, and Wang K L 2022 *Adv. Mater.* **34** 2105266
[5] Zhang Y Y, Ren X L, Liu R Z, Chen Z H, Wu X Z, Pang J, Wang W, Lan G B, Watanabe K, Taniguchi T, Shi Y G, Yu G Q, and Shao Q M 2024 arXiv:2405.06250 [cond-mat.mes-hall]
[6] Guo Y, Liu N S, Zhao Y Y, Jiang X, Zhou S, and Zhao J J 2020 *Chin. Phys. Lett.* **37** 107506
[7] Sivadas N, Okamoto S, Xu X D, Fennie C J, and Xiao D 2018 *Nano Lett.* **18** 7658
[8] Zhang P Y, Chung T F, Li Q W, Wang S Q, Wang Q J, Huey W L B, Yang S, Goldberger J E, Yao J, and Zhang X 2022 *Nat. Mater.* **21** 1373
[9] Gupta V, Cham T M, Stiehl G M, Bose A, Mittelstaedt J A, Kang K F, Jiang S W, Mak K F, Shan J, Buhrman R A, and Ralph D C 2020 *Nano Lett.* **20** 7482
[10] Hao Z Q, Li H W, Zhang S H, Li X T, Lin G T, Luo X, Sun Y P, Liu Z, and Wang Y Y 2018 *Sci. Bull.* **63** 825
[11] Zhu W X, Song C, Han L, Guo T W, Bai H, and Pan F 2022 *Nat. Commun.* **13** 6428
[12] Chen X H, Wang H T, Liu H J, Wang C, Wei G S, Fang C, Wang H C, Geng C Y, Liu S J, Li P Y, Yu H M, Zhao W S, Miao J G, Li Y T, Wang L, Nie T X, Zhao J M, and Wu X J 2022 *Adv. Mater.* **34** 2106172
[13] Deng Y J, Yu Y J, Song Y C, Zhang J Z, Wang N Z, Sun Z Y, Yi Y F, Wu Y Z, Wu S W, Zhu J Y, Wang J, Chen X H, and Zhang Y B 2018 *Nature* **563** 94
[14] Feng H L, Li Y, Shi Y G, Xie H Y, Li Y Q, and Xu Y 2022 *Chin. Phys. Lett.* **39** 077501
[15] Liu X Q, Huang P Y, Xia Y, Gao L, Liao L Y, Cui B S, Backes D, van der Laan G, Hesjedal T, Ji Y C, Chen P, Zhang Y F, Wu F, Wang M X, Zhang J W, Yu G Q, Song C, Chen Y L, Liu Z K, Yang Y M, Peng Y, Li G, Yao Q, and Kou X F 2023 *Adv. Funct. Mater.* **33** 2304454
[16] Xian J J, Wang C, Nie J H, Li R, Han M J, Lin J H, Zhang W H, Liu Z Y, Zhang Z M, Miao M P, Yi Y F, Wu S W, Chen X D, Han J B, Xia Z C, Ji W, and Fu Y S 2022 *Nat. Commun.* **13** 257
[17] Zhang X Q, Lu Q S, Liu W Q, Niu W, Sun J B, Cook J, Vaninger M, Miceli P F, Singh D J, Lian S W, Chang T R, He X Q, Du J, He L, Zhang R, Bian G, and Xu Y B 2021 *Nat. Commun.* **12** 2492
[18] Zhang G J, Guo F, Wu H, Wen X K, Yang L, Jin W, Zhang W F, and Chang H X 2022 *Nat. Commun.* **13** 5067
[19] Kajale S N, Nguyen T, Chao C A, Bono D C, Boonkird A, Li M D, and Sarkar D 2024 *Nat. Commun.* **15** 1485
[20] Pan Z C, Li D, Ye X G, Chen Z, Chen Z H, Wang A Q, Tian M L, Yao G J, Liu K H, and Liao Z M 2023 *Sci. Bull.* **68** 2743
[21] Zha H M, Li W, Zhang G J, Liu W J, Deng L W, Jiang Q, Ye M, Wu H, Chang H X, and Qiao S 2023 *Chin. Phys. Lett.* **40** 087501
[22] Zhu W K, Xie S H, Lin H L, Zhang G J, Wu H, Hu T G, Wang Z A, Zhang X M, Xu J H, Wang Y J, Zheng Y H, Yan F G, Zhang J, Zhao L X, Patané A, Zhang J, Chang H X, and Wang K Y 2022 *Chin. Phys. Lett.* **39** 128501